

An Anisotropic Fluid-Solid Model of the Mouse Heart

JP Carson¹, AP Kuprat¹, X Jiao², F del Pin³, DR Einstein¹

¹Pacific Northwest National Laboratory, Richland, WA, USA

²Stony Brook University, Stony Brook, NY, USA

³Livermore Software Technology Corporation, Livermore, CA, USA

Abstract

A critical challenge in biomechanical simulations is the spatial discretization of complex fluid-solid geometries created from imaging. This is especially important when dealing with Lagrangian interfaces, as there must be at a minimum both geometric and topological compatibility between fluid and solid phases, with exact matching of the interfacial nodes being highly desirable. We have developed a solution to this problem and applied the approach to the creation of a 3D fluid-solid mesh of the mouse heart. First, a 50 micron isotropic MRI dataset of a perfusion-fixed mouse heart was segmented into blood, tissue, and background using a customized multimaterial connected fuzzy thresholding algorithm. Then, a multimaterial marching cubes algorithm was applied to produce two compatible isosurfaces, one for the blood-tissue boundary and one for the tissue-background boundary. A multimaterial smoothing algorithm that rigorously conserves volume for each phase simultaneously smoothed the isosurfaces. Next we applied novel automated meshing algorithms to generate anisotropic hybrid meshes with the number of layers and the desired element anisotropy for each material as the only input parameters. As the meshes are scale-invariant within a material and include boundary layer prisms, fluid-structure interaction computations would have a relative error equilibrated over the entire mesh. The resulting model is highly detailed mesh representation of the mouse heart, including features such as chordae and coronary vasculature, that is also maximally efficient to produce the best simulation results for the computational resources available.

1. Introduction

The movement of blood is directly linked to cardiac health. Disturbances in flow can lead to thrombus formation and coronary obstruction. Inappropriate shear stresses can lead to the formation of atherosclerotic plaques. Treating the interface between the heart tissue material and the blood material in a Lagrangian framework allows fluid sheer stresses to be resolved more

accurately. To accomplish this requires that the grid for both materials can evolve over time separately, which is addressed in part in [1]. The other requirement is that the discretization of each material must be consistent at the boundary in spite of differences in the physical conditions driving the discretization of each material. This is the focus of the methods described here.

Our method uses a gradient-limited feature size metric calculated locally for each material to guide the adaptation of the surface mesh, the generation of a layered tetrahedral mesh for the solid material, the generation of the prismatic mesh at the boundary layer of the fluid material, and the generation of the tetrahedral mesh in the interior of the fluid material. Through this approach, scale-invariance is achieved such that even the smallest features – e.g., coronary vessels – are guaranteed to have a user-defined number of layers across the diameter. In addition, we laminate the cardiac tissue to seamlessly transition between myocardium, cardiac valves, and coronary lumen. The approach enables automated adaptation of the boundary layer by scale. The user only has to specify a few parameters – number of layers, degree of anisotropy, prism growth ratio, and range of allowable feature sizes – when automatically generating the mesh with this method.

2. Methods

2.1. Image volume segmentation

A 50 μm isotropic resolution magnetic resonance image volume (512 x 512 x 2048) of an actively stained adult male C56BL6 mouse was generated at the Duke Center for In Vivo Microscopy [2]. An 8-bit per voxel grayscale 249 x 216 x 240 volume subset encompassing the heart and nearby tissues was cropped from the total volume for segmentation.

Segmentation proceeded in four steps. For the first step, all voxels were initially automatically assigned to material types – blood material (M_b), disputed material (M_d), heart tissue material (M_h), and other non-cardiovasculature tissue material (M_o) – based on voxel intensity using thresholds of 150, 110, and 50

respectively. For the second step, all M_d voxels were reassigned to either M_h or M_b . 26-adjacency groups of M_d voxels which were completely encapsulated by a single material were automatically assigned to the encapsulating material. Then, M_d voxels representing coronary vasculature were automatically reassigned to M_b when the majority of the 26-adjacency neighborhood voxels were M_h . Remaining M_d voxels were highlighted in a graphical user interface (GUI) and visually evaluated for manual reassignment based on anatomical topology. For the third step, M_o was further assigned by masking the non-cardiovascular heart region of interest. This masking was semi-automated and utilized a warp function calculated by multiresolution elastic image registration [3] between adjacent images and applied to a user-defined initial image mask. For the final step, the topology of the segmentation was validated by iteratively applying the following events: setting M_o voxels that 26-adjacency touch M_b to be M_h ; highlight in the GUI and manually fix all same material voxels connected by 26-adjacency but not 6-adjacency; and reassign voxels so that there is only one main connected voxel component for each material type.

2.2. Mesh generation

The external tissue surface as the boundary between M_h and M_o , and the tissue-blood surface as the boundary between M_h and M_b were extracted from the image volume segmentation using a variant of the marching cubes algorithm [4]. Then we defined the raw feature size for each surface node as the local diameter represented by the length of the truncated line segment of the inward normal from the node to the first intersection [5]. This feature size was restricted using user-specified minimum and maximum scale-lengths. In small tubular sections of the surface, the feature size was further augmented by the radius of curvature [6] to guarantee a specified minimum number of nodes around the circumference. An outward raw feature size field was also calculated. The feature size fields were gradient limited to smooth the effects of abrupt changes [7]. We applied the feature size fields to the creation of scale-invariant refined high quality surface meshes using the operations of Rivara edge bisection, node merging, and edge swaps [5,7].

We achieved a computational grid mimicking lamination of cardiac tissue by creating layers of tetrahedral elements on the interior of the refined surface. Points were cast along the normal of the surface and connected with a layer-aware Delaunay algorithm [5]. Duplicated points were filtered and tetrahedra containing no interior points were removed. The tetrahedral grid was improved via layer-aware edge-flipping operations and sliver removal operations similar to [8].

We then created the blood volumetric mesh starting

with a prismatic boundary layer by advancing the surface layer using the face offsetting method [9], applying a variational smoothing procedure to improve element shapes [7], and using the gradient limited feature size of the surface as the speed function. Then the remaining space of the interior of the blood volume was tetrahedralized using the boundary constrained Delaunay method in TetGen [10].

3. Results

The mouse heart dataset was successfully segmented into the material components and from these an anisotropic volumetric multi-material mesh suitable for fluid-solid simulation was generated. Figure 1A shows an example cropped image from the MR dataset. Figure 1B depicts the same image after segmentation. Figure 1C and 1D illustrate the exterior heart surface and the heart-blood surface respectively, with the surfaces highlighted in color by the featuresize at the various surface locations. The final volumetric mesh of the dataset is shown in Figure 1E (whole heart), 1F (blood material), and 1G (tissue material). In total, the heart tissue had 15,571,963 tetrahedra, while the blood mesh had 6,882,265 prisms and 5,735,350 tetrahedra. The mesh quality achieved for the dataset was excellent. The mesh quality for tetrahedra was measured using *aspect ratio* (ranging from 0 to 1 with 1 representing the ideal shape) which was greater than 0.1 for 99.99% of the tetrahedra. The mesh quality for prisms was measured using a *scaled aspect ratio* [7] (also ranging from 0 to 1 with 1 representing the ideal shape) which was greater than 0.2 for 99.999% of the prisms.

4. Discussion and conclusions

Connecting biomedical modelling to imaging data not only provides geometric information, but can also help place physiological data into the context of the model. Such biomedical based geometries are highly complex which has previously limited their adoption in biomedical computations. Efficient unstructured mesh generation adapted to the particular physics of the biological material is a challenge. Though computational power continuously increases, these resources must still be used intelligently to minimize computational cost and discretization error. This requires adapting the geometry appropriately while maintaining grid organization suitable to the material properties.

Such challenges are not limited to the heart, though the heart does pose some unique challenges. The first of these is the profound effects of blood flow on cardiac mechanics and physiology. The critical nature of the fluid-solid interface dictates accurate resolution of the continuum fields. In other work we have presented the

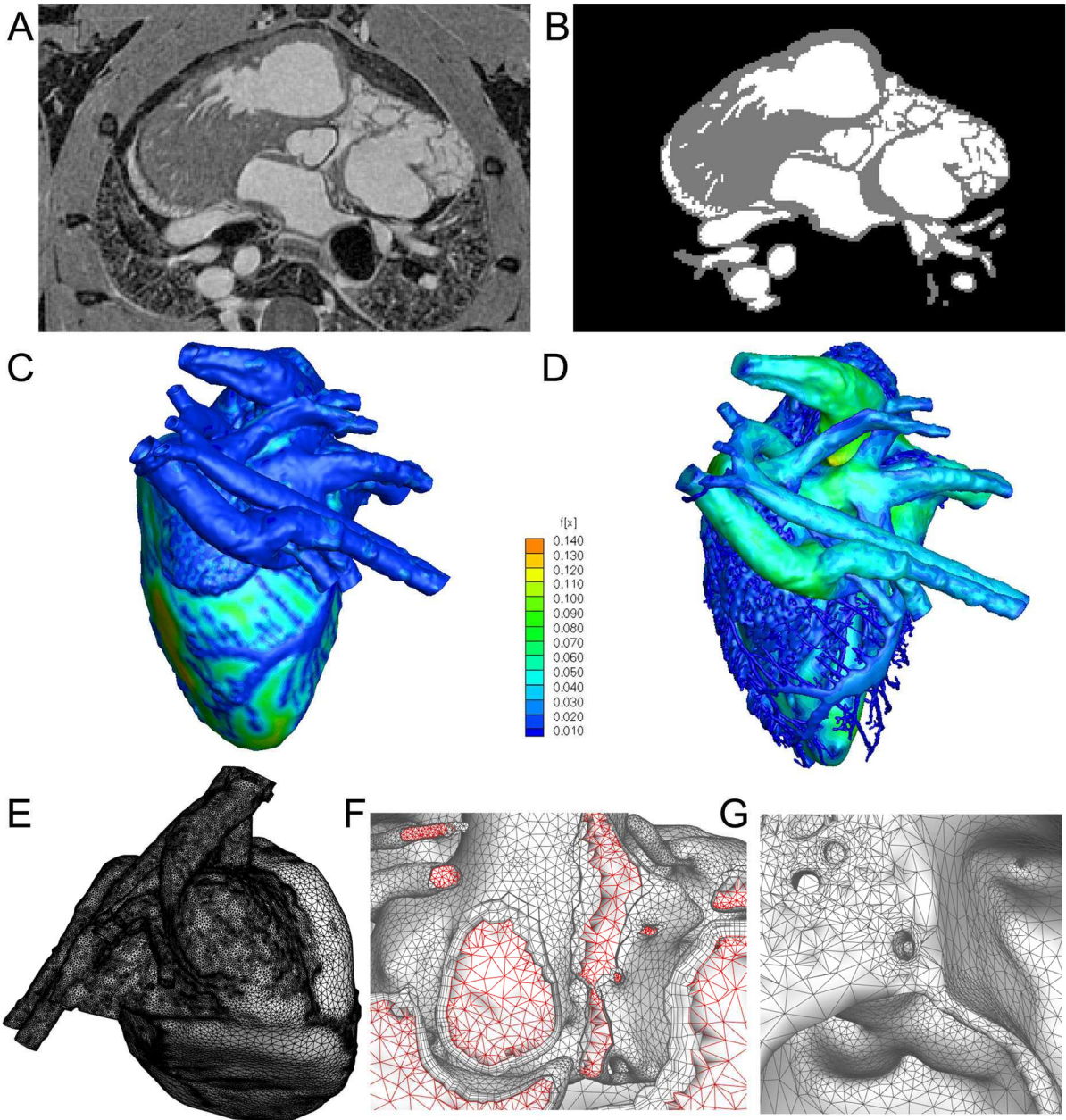


Figure 1. Generating the anisotropic fluid-solid model of the mouse heart. A) Example slice of MR image. B) Final segmentation of example image shows heart tissue in grey, blood material in white, and other material in black. C) Exterior surface of tissue material colored by featuresize. D) Surface of the blood material colored by featuresize. E) View of exterior of final volumetric mesh. F) Cutaway of volume mesh of blood material shows hybrid nature of prisms and tetrahedra. G) Cutaway of heart tissue mesh which is purely tetrahedral.

numerical framework to accomplish a Lagrangian treatment of tissue-blood interfaces [1]. The second of these challenges is that most heart structures cannot be approximated by a plane-stress membrane assumption,

implying the explicit discretization with volume elements such as tetrahedral, hexahedra, and prisms.

Here we have presented our method for computing high-quality scale-invariant grids that is applicable to a

wide variety of multimaterial data sets. A more detailed description of our methods including pseudocode will be available in [11]. We have demonstrated our approach on a highly detailed MRI dataset of the *in situ* mouse heart. The excellent mesh quality achieved, as indicated by aspect ratios, is due to topologically correct segmentation to produce surface meshes, the use of gradient-limited feature size fields, and variational optimization of prisms based on the face-offsetting method.

The efficient computation of the gradient-limited feature size field allows the concept of scale to be incorporated into all aspects of our mesh generation methods. In this way, the number of elements is reduced by 2-3 orders of magnitude from that which would be required using geometry-independent meshing approaches to capture the smallest structures in computable detail. Adoption of the gradient-limited feature size allows efficient placement of mesh only where it is needed. Other savings are achieved by decoupling tangential and normal directions for mesh density. In addition, scale-invariant layering allows a valid mesh to be maintained for a longer period of time in areas of large deformation.

Future work will primarily focus on the following four areas of improvement. The first area of improvement is to optimize the grid in locations such as chordae and coronary arteries to utilize anisotropic gridding with higher densities in the direction with the highest curvature. Currently, the grid density tangential to the surface is isotropic. The second area of improvement is relaxing the constrained Delaunay tetrahedralization requirement in the core of the fluid material region. Delaunay tetrahedralization can limit the quality of the tetrahedral core for some complex geometries. Though our discretization in this zone is preliminary – the discretization will evolve with the adaptation in the fluid solver driven by an error metric – the initial interior grid quality is still important. The third area of improvement is the development of a robust volume conserving smoothing algorithm that guarantees against self-intersections. Our current volume conserving smoothing [12] has the advantage of over conventional smoothing approaches by constraining volume and limiting drift. However it must be applied with care as it does not guarantee against self intersections. Self intersections would create invalid surfaces and prevent the additional volumetric meshing steps from being appropriately applied. The fourth area of improvement is the use of the face-offsetting method as a discretization tool. This will allow select nodes to merge, collapsing prisms into a small number of pyramids and tetrahedra.

Acknowledgements

The MR data was supplied by Dr. G. Allan Johnson, Duke Center for In Vivo Microscopy under support from NCRR/NCI (P41 RR05959/U24 CA092656). The work described in this paper was funded by the National Heart Lung and Blood Institute Awards 1RO1HL073598-01A1 and 1R01HL084431-01A1, by the National Science Foundation under award number DMS-0809285, and by the U.S Department of Energy under LDRD DE-AC05-76RL01830.

References

- [1] Einstein DR, del Pin F, Kuprat AP, Jiao X, Carson JP, Kunzleman KS, Cochran RP, Guccione J, Ratcliffe M. Fluid-structure interactions of the mitral valve and left heart: comprehensive strategies, past, present and future. *Comm in Num Meth in Eng* 2009; in press.
- [2] Johnson GA, Cofer GP, Gewalt SL, Hedlund LW. Morphologic phenotyping with MR microscopy: the visible mouse. *Radiology* 2002;222:789-93.
- [3] Kostec P, Weaver J, Healy D. Multiresolution elastic image registration. *Medical Physics* 1998;25:1593-604.
- [4] Treece GM, Prager RW, Gee AH. Regularised marching tetrahedral: improved iso-surface extraction. *Computers & Graphics* 1991;23:583-98.
- [5] Kuprat AP, Einstein DR. An anisotropic scale-invariant unstructured mesh generator suitable for volumetric imaging data. *J Comput Phys* 2009;228:619-40.
- [6] Jiao X, Zha H. Consistent computation of first- and second-order differential quantities for surface meshes. In SPM 2008. New York: ACM, 2008:159-70.
- [7] Dyedov V, Einstein DR, Jiao X, Kuprat AP, Carson JP, del Pin F. Variational generation of prismatic boundary-layer meshes. *Int J Num Meth Eng* 2009;79:907-45.
- [8] Moyle KR, Ventikos Y. Local remeshing for large amplitude grid deformations. *J Comput Phys* 2008; 227:2781-93.
- [9] Jiao X. Face offsetting: a unified approach for explicit moving interfaces. *J Comput Phys* 2007;220:612-25.
- [10] Si H. Adaptive tetrahedral mesh generation by constrained Delaunay refinement. *Int J Num Meth Eng* 2008;75:856-80.
- [11] Carson JP, Kuprat AP, Jiao X, Dyedov V, Guccione JM, Ratcliffe MB, Einstein DR. Adaptive generation of multimaterial grids from imaging data for biomedical structure simulations. *Biomechanics and Modeling in Mechanobiology* 2009;in press.
- [12] Kuprat A, Khamayseh A, George D, Larkey L. Volume conserving smoothing for piecewise linear curves, surfaces, and triple lines. *J Comput Phys* 2001;172:99-118.

Address for correspondence

James P. Carson
P.O. Box 999, MSIN P7-58, Richland, WA 99352
james.carson@pnl.gov